Behavioral/Cognitive

A Scaffold for Efficiency in the Human Brain

Agnieszka Z. Burzynska,[1,2]* Douglas D. Garrett,[1,3]* Claudia Preuschhof,[4] Irene E. Nagel,[4] Shu-Chen Li,[1,5] Lars Bäckman,[6] Hauke R. Heekeren,[1,4,7] and Ulman Lindenberger[1]

[1]Center for Lifespan Psychology, Max Planck Institute for Human Development, 14195 Berlin, Germany, [2]Beckman Institute for Advanced Science and Technology, University of Illinois, Urbana, Illinois 61820, [3]Wellcome Trust Centre for Neuroimaging, Institute of Neurology, University College London, London, WC1N 3BG, United Kingdom, [4]Department of Education and Psychology, Freie Universität Berlin, 14195 Berlin, Germany, [5]Department of Psychology, TU Dresden, 01062 Dresden, Germany, [6]Aging Research Center, Karolinska Institute, SE-113 30 Stockholm, Sweden, and [7]Max Planck Institute for Human Cognitive and Brain Sciences, 04103 Leipzig, Germany

The comprehensive relations between healthy adult human brain white matter (WM) microstructure and gray matter (GM) function, and their joint relations to cognitive performance, remain poorly understood. We investigated these associations in 27 younger and 28 older healthy adults by linking diffusion tensor imaging (DTI) with functional magnetic resonance imaging (fMRI) data collected during an n-back working memory task. We present a novel application of multivariate Partial Least Squares (PLS) analysis that permitted the simultaneous modeling of relations between WM integrity values from all major WM tracts and patterns of condition-related BOLD signal across all GM regions. Our results indicate that greater microstructural integrity of the major WM tracts was negatively related to condition-related blood oxygenation level-dependent (BOLD) signal in task-positive GM regions. This negative relationship suggests that better quality of structural connections allows for more efficient use of task-related GM processing resources. Individuals with more intact WM further showed greater BOLD signal increases in typical "task-negative" regions during fixation, and notably exhibited a balanced magnitude of BOLD response across task-positive and -negative states. Structure—function relations also predicted task performance, including accuracy and speed of responding. Finally, structure–function–behavior relations reflected individual differences over and above chronological age. Our findings provide evidence for the role of WM microstructure as a scaffold for the context-relevant utilization of GM regions.

Introduction

Cognitive performance necessarily relies on the integrity of white matter (WM) fibers (that provide a skeleton for neural signal transmission), and the quality of neural processing in gray matter (GM). However, the specific relations between WM microstructure and GM functioning in the healthy adult brain, and their joint relations to cognitive abilities, remain understudied. Although better structural connectivity is linked to higher cognitive functioning (Johansen-Berg, 2010; Burzynska et al., 2011; Fjell et al., 2011; Madden et al., 2012), it is unclear whether greater WM integrity is associated with higher or lower GM activity, and how this relation is modulated within regions activated on ("task-positive") and off ("task-negative") task (Fox et al., 2005; Buckner et al., 2008; Raichle, 2010).

Many functional neuroimaging studies suggest that better performers require less brain activity (relative to baseline) to successfully perform a task of a given difficulty level (Neubauer and Fink, 2009). Convergent with neural efficiency theory (Haier et al., 1988), fast-performing young adults often show lower and less extensive activity than slow performers in select task-positive regions, such as dorsal lateral prefrontal cortex (Rypma and D'Esposito, 1999; Rypma et al., 2002). Sparsely available univariate studies on healthy older adults report negative relations between structural integrity in restricted regions in WM and neural activity in task-positive frontoparietal regions (Persson et al., 2006; Madden et al., 2007; Schulze et al., 2011). However, the role of WM integrity in global, whole-brain processing efficiency is still unknown. We predict that greater WM integrity should generally be linked to lower (more efficient) brain activity in task-positive regions. Conversely, the exact opposite effect may exist between WM integrity and the magnitude of "task-negative" activity at fixation. Canonical task-negative (default mode) regions are typically more active during fixation relative to task (and thus, these same regions are necessarily "deactivated" on task), a phenomenon that is reduced in poorer performers, older adults, and especially in those with dementia (Lustig et al., 2003; Grady et al., 2006, 2010; Sperling et al., 2009; Sambataro et al., 2010). Given known links between cognitive performance, aging, and WM integrity (for a review, see Madden et al., 2012), those with high WM integrity may also have higher activation magnitude in task-

Received April 1, 2013; revised Sept. 6, 2013; accepted Sept. 16, 2013.

Author contributions: A.Z.B., D.D.G., S.-C.L., L.B., H.R.H., and U.L. designed research; A.Z.B., C.P., and I.E.N. performed research; D.D.G. contributed unpublished reagents/analytic tools; A.Z.B. and D.D.G. analyzed data; A.Z.B. and D.D.G. wrote the paper.

D.D.G and U.L. were partially supported by the Max Planck Society-University College London Initiative for Computational Psychiatry and Ageing Research (ICPAR). L.B. was supported by grants from the Swedish Research Council and Swedish Brain Power, an Alexander von Humboldt Research Award, and by a donation from the af Jochnick Foundation. We thank Janina Marchner, Steffen Wiegert, and Concepcion Padilla for help with data analyses.

*A.Z.B. and D.D.G. contributed equally to this work.

The authors declare no competing financial interests.

Correspondence should be addressed to Agnieszka Z. Burzynska, Lifelong Brain and Cognition Lab, Beckman Institute for Advanced Science and Technology, University of Illinois, 405 N Mathews Avenue, Urbana, IL 61820. E-mail: agaburza@illinois.edu.

DOI:10.1523/JNEUROSCI.1426-13.2013

 0270-6474/13/3317150-10$15.00/0

negative regions during fixation. Accordingly, higher WM integrity should promote a clearer differentiation in BOLD signal between fixation and task in typical task-negative regions.

To test these hypotheses we combined diffusion tensor imaging and working-memory fMRI data from a sample of 55 healthy adults. Using a novel application of multivariate Partial Least Squares [PLS (McIntosh et al., 1996)], we simultaneously modeled the relations between all major WM tracts and whole-GM patterns of condition-related neural activity. We then examined the covariation between these multivariate effects and cognitive performance. Detecting robust structure—function relationships required a sample with a sufficiently broad distribution of WM integrity, fMRI, and behavioral data. Thus, we recruited younger and older adults, as normal aging magnifies individual heterogeneity in healthy adult lifespan samples (Nyberg et al., 2012; Lindenberger et al., 2013). Finally, as chronological age is an indirect proxy for both neural and non-neural factors, we further predicted that WM structure-GM function relations and WM–GM effects on cognitive performance would not be fully accounted for by age group.

Materials and Methods

Participants

The sample consisted of 27 younger (YA; age range 20–31, mean ± SD 24.3 ± 3.2, 14 female, years of education 16.4 ± 3.1) and 28 older (OA; age range 60–70, mean ± SD 63.2 ± 2.5, 13 female, years of education 15.4 ± 3.8) adults. The current participants were a subsample of participants recruited for prior studies (Burzynska et al., 2011; Nagel et al., 2011), from whom high quality diffusion tensor imaging (DTI) and fMRI data were available. All participants were right-handed, with normal or corrected-to-normal vision, and reported to be psychiatrically and neurologically healthy. Participants showed age-typical performance levels on measures of perceptual speed (items completed in Digit-Symbol Substitution; YA: 64.4 ± 11.4; OA: 49.1 ± 10.0; $p < 0.001$) and verbal knowledge (correct responses on the Spot-a-Word task; YA: 18.9 ± 4.7 OA: 22.8 ± 6.3; $p = 0.012$). All OA were nondemented, community dwelling, and scored >25 points on the Mini Mental Status Examination. The Ethics Committee of the Charité University Medicine Berlin approved the study, and written informed consent was obtained from all participants. All of them received financial reimbursement.

MRI acquisition and analysis

DTI. DTI allows inferences about WM microstructure *in vivo* by quantifying the magnitude and directionality of diffusion of water within a tissue (Beaulieu, 2002). Fractional anisotropy (FA), a measure of the directional dependence of diffusion, reflects the level of WM integrity within a voxel [i.e., fiber size, density, coherence, degree of myelination, and myelin integrity (Beaulieu, 2002)], in which higher FA serves as a proxy measure of faster and more reliable information transfer along axons.

We acquired DTI images on a 1.5 T Siemens Sonata with 40 mT/m gradients and 200 T/m/s slew rates (Siemens) on average 57 d after our fMRI data collection. All images were obtained parallel to the anterior–posterior commissure plane with no interslice gap. Eddy current-induced image distortions were minimized by using a twice-refocused spin echo single-shot Echo Planar Imaging sequence (Reese et al., 2003), with TR/TE = 8500/96 ms, 128 × 128 matrix, 2.5 mm^2 in-plane resolution, and receiver bandwidth of 1502 Hz, comprising 52 2.5-mm-thick slices. The protocol consisted of a set of 12 noncollinear diffusion-weighted acquisitions, with b-value = 1000 s/mm^2 and a T2-weighted, b-value = 0 s/mm^2 acquisition, each repeated four times.

DTI data were processed using the FSL 4.1 Diffusion Toolbox (FDT: http://www.fmrib.ox.ac.uk/fsl) in a standard multistep procedure, including: (1) motion and eddy current correction of the images and corresponding b-vectors, (2) removal of the skull and nonbrain tissue using the Brain Extraction Tool (Smith, 2002), and (3) voxel-by-voxel calculation of the diffusion tensors. Using the diffusion tensor information, FA maps were computed using DTIFit.

We used TBSS v1.2 (Smith et al., 2006, 2007), a toolbox within FSL (Smith et al., 2004), to create a representation of main WM tracts common to all participants (WM "skeleton"). This included: (1) nonlinear alignment of each participant's FA volume to the 1 × 1 × 1 mm^3 standard Montreal Neurological Institute (MNI152) space via the FMRIB58_FA template using the FMRIB's Nonlinear Registration Tool [FNIRT (Rueckert et al., 1999); http://www.doc.ic.ac.uk/~dr/software], (2) calculation of the mean of all aligned FA images, (3) creation of the WM skeleton by perpendicular nonmaximum-suppression of the mean FA image and setting the FA threshold to 0.25, and (4) perpendicular projection of the highest FA value (local center of the tract) onto the skeleton, separately for each participant.

To obtain the measure of global WM integrity, we averaged the FA values from the entire skeleton for each participant (global FA). To verify how different tracts contribute to the multivariate structure—function relationships, we extracted mean FA values from 22 regions (Fig. 1*A*) representing core parts of main association, projection, and commissural fibers. The regions were identified on the TBSS skeleton using the DTI white-matter atlas (Mori et al., 2005).

Functional MRI. While undergoing fMRI, participants performed a letter n-back task adjusted to reduce switch costs in older participants (Nagel et al., 2011). A series of letters was presented and the task was to compare the currently presented letter with the letter seen one, two, or three letters earlier (1-, 2- and 3-back conditions, respectively). We acquired three runs for each participant, where each run consisted of two successive blocks of each condition (a blocked-design), all alternating between 20-s-long fixation blocks. The order of conditions was different in each run. Fifteen letters were presented during each condition block and therefore there were 14 1-back trials, 13 2-back trials, and 12 3-back trials in each block (total number of trials was 84, 78, and 72, respectively). Each block began with 5000 ms presentation of the condition cue (1-, 2-, or 3-back). Each letter stimulus was presented for 1500 ms, separated by a 500 ms fixation cross (total of 14 fixation crosses was presented in each block). Participants responded "yes" (i.e., the current letter is the same as the n-back letter) or "no" (the current letter is not the same as n-back letter) with a button press. Before entering the scanner, participants were verbally instructed about the task, practiced three runs, and received feedback on their performance. N-back performance in the scanner was assessed by percentage of correct responses, including both hits and correct rejections, to best represent performance across each task block (accuracy) and by the average response latency during correct trials [reaction time (RT)]. Trials of RT < 200 ms were excluded.

Whole-brain functional MRI data were collected using a 1.5 T Siemens Vision MRI system with a standard EPI sequence (TR/TE = 2500/40 ms, flip angle 90°, voxel size 4 × 4 × 4.6 mm^3, interslice gap 0.15, 26 slices acquired in ascending order approximately axial to the bicommissural plane). Three dummy volumes preceded each of the three experimental runs to achieve a steady state of tissue magnetization. Each run lasted ~5 min. Two structural scans (proton-density-weighted sequence: TR/TE = 4350/15 ms; flip angle 180°; 252 × 256 matrix; 1 × 1 × 4 mm voxel size, and a sagitally oriented high resolution T1-weighted sequence: TR/TE = 20/5 ms; flip angle 30°; matrix 256 × 256; voxel size 1 mm^3) were acquired in the same orientation as the functional EPIs to aid coregistration of the functional images.

fMRI data were preprocessed with FSL 4.1 (Smith et al., 2004). Preprocessing included the following: motion-correction with spatial smoothing (8 mm full-width at half-maximum Gaussian kernel), high-pass filtering (σ = 108 s), and modeling of intrinsic autocorrelations using prewhitening. Registration of functional images to high-resolution participant-specific T1 images, and from T1 to standard space (MNI 152_T1) was performed using FLIRT (Jenkinson and Smith, 2001; Jenkinson et al., 2002), followed by further refinement of registration of high resolution structural to standard MNI 152_T1 space using FNIRT nonlinear registration (Andersson et al., 2007). The registration matrices were then used to transform the functional data of each run to the MNI 152_T1 template. To restrict all multivariate analyses to the GM, we masked our functional data with the GM tissue prior provided in FSL, thresholded at probability >0.37. Our blocked-design BOLD signal was expressed as a percent change within an entire block (task or fixation)

from the mean of the final three scans of the preceding block. Referring to the preceding block effectively acts as a local high-pass filter on the data, avoiding the need to detrend. To calculate mean BOLD signals for each voxel and experimental condition, we averaged mean percent change within each block across all blocks for a given condition.

Blocked-designs necessarily involve examining condition-based BOLD data without differentiating into correct and incorrect trials. This design was most suitable for the current study as we were interested in BOLD signal reflecting average sustained brain activity for a given working memory load (and its relations to WM integrity and task performance), rather than single trial activity. In addition, trial length increased with task difficulty, resulting in different numbers of total trials (1-back > 2-back > 3back). Excluding incorrect trials (or blocks containing them) would further increase the disproportion in number of trials between conditions. Importantly, although we did observe the expected decrease in accuracy from 1- to 3-back (see Results), even older adults performed well above chance level during 3-back. Therefore, we expect that the measured BOLD signal reflected continuous encoding and maintenance of items in working memory in the vast majority of blocks. However, precisely how structure–function–behavior relations differ between correct and incorrect trails requires investigation within an event-related design, which we do not pursue here. Future studies using imaging techniques with higher temporal resolution (e.g., EEG) may also help tease apart structure—function relations with respect to different processes underlying working memory performance, such as encoding, maintenance, and retrieval.

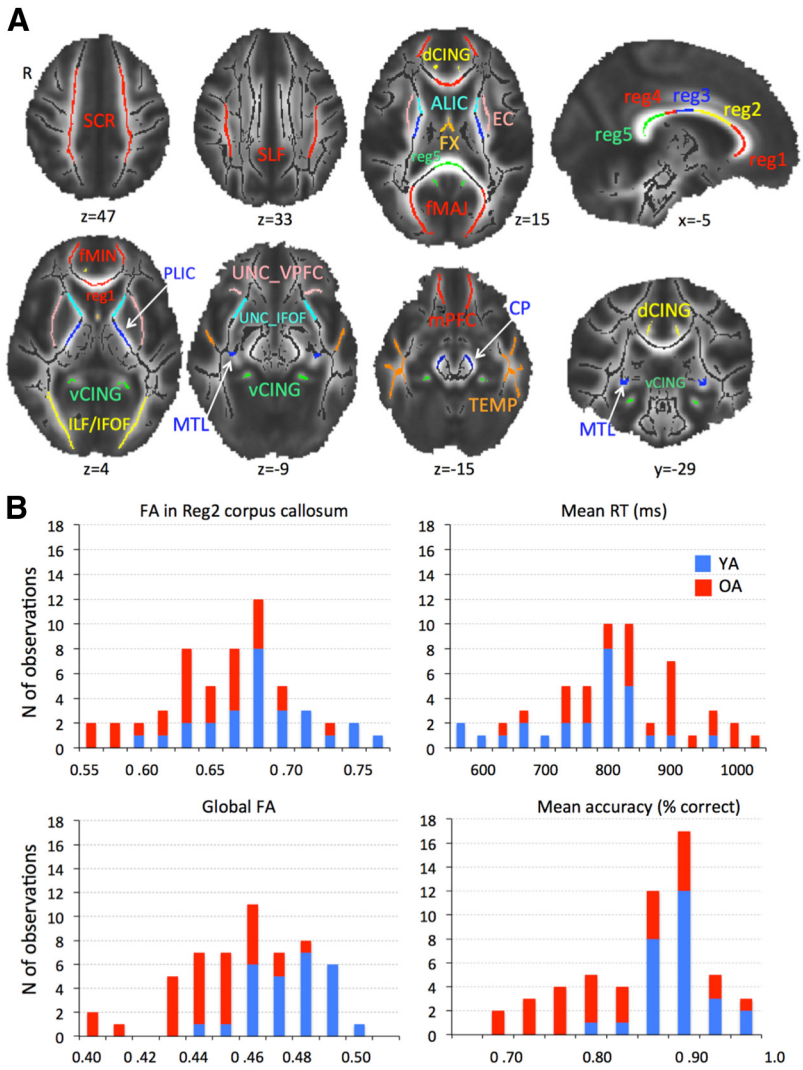

Figure 1. ***A***, WM regions of interest. Superior corona radiata (SCR), superior longitudinal fasciculus (SLF), anterior and posterior limb of the internal capsule (ALIC and PLIC), external capsule (EC), fornix (FX), 5 regions of the corpus callosum [reg1, 2, 3, 4, 5 (Hofer and Frahm, 2006)], forceps major (fMAJ), forceps minor (fMIN), dorsal (dCING), and ventral cingulum (vCING), WM containing occipital portion of inferior longitudinal fasciculi and inferior fronto-occipital fasciculi (ILF/IFOF), ventral prefrontal part of uncinate (UNC_VPFC), WM containing uncinate and inferior fronto-occipital fasciculi (UNC_IFOF), medial temporal lobe WM (MTL), WM of the medial PFC (mPFC), WM of the temporal pole related to inferior longitudinal fasciculus (TEMP), and cerebral peduncles (CP). ***B***, Histograms of region 2 of corpus callosum and global FA, mean RT, and mean accuracy in YA and OA. Note the overlapping distributions despite mean group differences.

PLS multivariate analysis of relations among FA, BOLD signal, and age group

Our sample included both younger and older adults to ensure sufficient range of individual differences in FA values and n-back performance. As depicted in Figure 1*B*, the distributions of FA and behavioral measures were unimodal and overlapping for the combined YA and OA sample. This indicates that both the WM integrity and behavioral data represent a continuum across adulthood, and splitting the sample based only on age group would be artificial from both biological and statistical perspectives. We therefore considered our participants as a single sample for various analyses of links between WM, BOLD, and performance. To account for any covariation among the measures of interest and age, we also tested possible effects of age group using several subsequent analyses (see below).

To identify multivariate patterns of relations between WM integrity and GM functional activity, we performed behavioral PLS analysis (McIntosh et al., 1996; Krishnan et al., 2011). This approach permits the analysis of the relations between FA from all major WM tracts and BOLD signal in all GM regions in one model, without the need of restricting the analyses to specific regions-of-interest. The behavioral PLS analysis begins with a correlation matrix (CORR) between our variables of interest (FA values from 22 WM regions and global FA) and each voxel's signal on each task condition (1-, 2-, 3-back, and fixation); correlations are calculated across participants. Then, this CORR matrix is decomposed via singular value decomposition (SVD):

$$SVD_{CORR} = USV' \quad (1)$$

This decomposition produces a left singular vector of FA weights (U), a right singular vector of BOLD weights (V), and a diagonal matrix of singular values (S). In other words, this analysis produces orthogonal latent variables (LVs) that optimally represent relations between FA values and BOLD in GM voxels. Each LV contains a spatial pattern depicting the brain regions where the activity shows the strongest relation to FA. To obtain a summary measure of each participant's expression of a particular LV pattern, we calculated within-person "brain scores" by multiplying each voxel's (i) weight (V) from each LV (j) produced from the SVD in Equation 1 by the BOLD value in that voxel for person (k), and summing over all (n) brain voxels:

$$\sum_{i=1}^{n} V_{ij}\,\mathrm{BOLD}_{ik} \quad (2)$$

Thus, in a single measure, a brain score indicates the degree to which a participant expresses the multivariate spatial pattern captured by a given

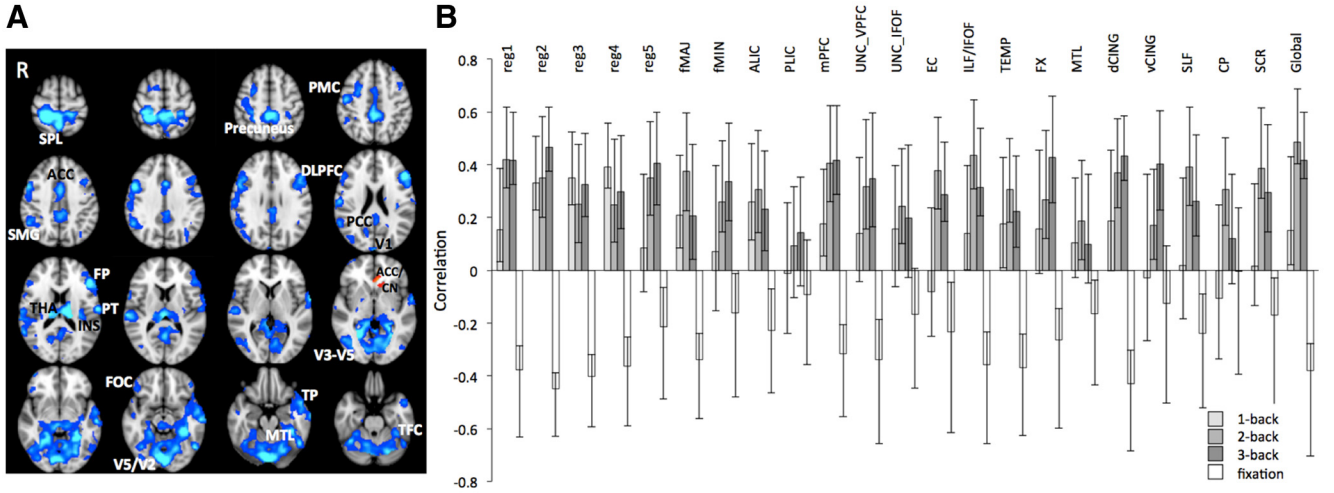

Figure 2. Multivariate relationships between WM integrity and BOLD signal. ***A***, Spatial pattern where higher FA was related to less BOLD signal during task but more BOLD signal during fixation (blue-light blue). Only in one small cluster higher FA was related to higher BOLD signal at task and lower at fixation (red). Significant regions: bootstrap ratio $> \pm 3$. PCC, Posterior cingulate cortex; DLPFC, dorsolateral prefrontal cortex; other labels are listed in Table 1. ***B***, Correlation magnitudes (Pearson *r*) between FA in the 23 WM regions and BOLD signal during 1-, 2-, 3-back, and fixation (permuted $p < 0.001$, error bars represent bootstrapped 95% confidence intervals).

FA-driven latent variable. Significance of detected relations between multivariate spatial patterns and experimental conditions was assessed using 1000 permutation tests of the singular value corresponding to each LV. A subsequent bootstrapping procedure revealed the robustness of voxel saliences across 1000 bootstrapped resamples of our data (Efron and Tibshirani, 1993). By dividing each voxel's mean salience by its bootstrapped SE, we obtained "bootstrap ratios" as normalized estimates of robustness. We thresholded bootstrap ratios at a value of ≥ 3.00, which approximates a 99% confidence interval. Because we examined FA values from 23 regions across four conditions, 92 LVs were possible.

To test whether the observed structure—function relationships were fully collinear with the effects of age group on WM integrity, we performed a separate behavioral PLS analysis relating age group (YA vs OA) to BOLD activity. This single variable (age group) examined across four conditions yielded four possible LVs.

To identify regions involved during fixation and task, we performed a separate mean-centering task PLS analysis (McIntosh et al., 1996; McIntosh and Lobaugh, 2004; Krishnan et al., 2011) that examined differences in BOLD signal between fixation, 1-, 2-, and 3-back conditions (again, four LVs possible). Akin to the behavioral PLS described above, task PLS looks at how brain activity covaries with our experimental conditions. This analysis was further used to put the multivariate pattern of structure—function relationships in the context of working memory- and fixation-related modulations in BOLD signal (see Results for more details).

General linear model analyses

All other statistical analyses were performed using SPSS (v.16, SPSS). The values reported in correlations or general linear model analyses were winsorized with respect to the distribution of the whole sample (2.5 ± SD) to reduce the effect of outliers. We used various general linear models to investigate the relationships between FA, BOLD, behavioral measures, and age group. For each model, we calculated Cook's Distance, which reflects the extent to which model residuals would change if a particular data point (in multivariate space) were excluded from the regression coefficient calculation. Larger Cook's Distance values indicate more influential data points. The threshold for determining influential observations was set according to previous recommendations [=4/number of observations (Bollen and Jackman, 1990)]. In the current study, the number of observations was 55, yielding a Cook's Distance threshold of 0.07; observations exceeding this threshold were deemed overly influential to our model results, and were thus removed from the data, with the additional constraint that not more than three cases per model were excluded (~5% of the total sample).

Results

Whole-brain structure—function relationships

Our multivariate analysis of FA-BOLD relations yielded one significant latent variable (permuted $p < 0.001$, 63.62% crossblock covariance), suggesting that higher FA was related to lower BOLD signal during task and higher BOLD signal during fixation periods, in multiple regions (Fig. 2*A*; the corresponding analyses within each age group yielded the same general direction of correlations and multivariate spatial pattern). Importantly, the correlation bars in Figure 2*B* indicate that, despite few nonsignificant correlations (i.e., 95% bootstrapped confidence intervals that crossed zero), structure—function relationships were consistent across all conditions and WM tracts. Only FA of the PLIC did not significantly contribute to the observed FA-BOLD correlation pattern. Of the remaining 22 FA ROIs, the relationship between FA and BOLD was always significant in the 2-back condition, significant in 19 ROIs for the 3-back condition, and in nine ROIs for the 1-back condition. This suggests that structure—function relationships, for most WM tracts, were stronger when the task involved sufficient working memory challenge (i.e., 2- and 3-back compared with 1-back) or when not engaging in the external task (during fixation). Peak voxels' location and reliability (bootstrap ratios) are reported in Table 1.

Contribution of age group to the FA-BOLD relationship

As there are well documented differences in FA between younger and older adults (Burzynska et al., 2010; Madden et al., 2012), we further investigated the contribution of age group to the FA-BOLD relationship. To this end, we compared the FA-BOLD model described above to a behavioral PLS model in which age group (YA vs OA) was linked to BOLD activity. Only the first LV was significant ($p < 0.001$, 74.76% crossblock covariance). We then overlaid the FA-BOLD and age group-BOLD patterns to examine similarities and differences (Fig. 3*A*). In many regions, such as right premotor cortex, parts of anterior cingulate, thalamus, ventral posterior cingulate gyrus, temporal pole, medial temporal lobe, and both primary and higher visual regions, only FA-BOLD relationships were significant (Fig. 3*B*, blue regions). Age group model-only regions (Fig. 3*B*, red) were far less prevalent and represented by clusters in supramar-

Table 1. Peaks, coordinates, bootstrap ratios, and cluster sizes for the PLS models

Model	Region	HEM	MNI coordinates			BSR	Cluster size (voxels)
			X	*Y*	*Z*		
FA-BOLD	Visual cortex (V5/V2)	L	−2	−86	−14	−7.59	20713
	Superior parietal lobule (SPL)	R	28	−40	62	−7.15	7425
	Thalamus (THA)	L	−14	−18	18	−6.12	438
	Planum temporale (PT)	R	64	−26	12	−5.06	1493
	Anterior cingulate cortex (ACC)	L	−2	14	36	−5.00	328
	Temporal pole (TP)	R	50	2	−46	−4.73	32
	Visual cortex (V1)	L/R	0	−94	22	−4.55	60
	Insular cortex (INS)	L	−32	−22	18	−4.37	198
	Frontal orbital cortex (FOC)	R	44	34	−18	−4.35	189
	Temporal fusiform cortex (TFC)	R	40	−8	−42	−4.28	100
	Frontal pole (FP)	R	42	58	−8	−4.23	56
	Visual cortex (V3-V5)	L	−36	−70	36	−4.22	94
	Premotor cortex (PMC)	R	28	0	48	−4.21	364
	Frontal Pole (FP)	L	−46	40	−14	−4.02	36
	Medial temporal lobe (MTL)	R	18	−14	−34	−4.00	60
	Temporal fusiform cortex (TFC)	L	−30	−14	−40	−3.65	12
	Pons	R	6	−34	−36	−3.51	20
	Insular cortex (INS)	R	30	−28	18	−3.51	29
	Pallidum	R	18	0	−4	−3.51	37
	Middle temporal gyrus	R	52	−8	−16	−3.48	60
	Frontal Pole	L	−32	40	46	−3.46	11
	Supramarginal gyrus (SMG)	L	−44	−52	30	−3.40	26
	Visual cortex (V3-V5)	L	−48	−78	−8	−3.36	69
	Temporal pole (TP)	R	54	14	−14	−3.29	12
	Pallidum	R	26	−16	−6	−3.24	19
	Middle temporal gyrus	L	−64	−58	6	−3.19	16
	Angular gyrus	R	40	−58	18	−3.12	14
	Anterior cingulate cortex/caudate nucleus (ACC/CN)	L	−4	30	−2	4.18	86
Age group-BOLD	Precuneus	L	−4	−36	50	7.75	7189
	Dorsolateral prefrontal cortex	L	−46	28	14	7.20	1486
	Temporal fusiform cortex	L	−34	−10	−40	6.89	1066
	Visual cortex V1	R	12	−76	−24	6.48	4083
	Dorsolateral prefrontal cortex	R	58	12	10	6.16	1414
	Temporal pole	R	50	2	−46	5.63	21
	Frontal Pole (FP)	L	−38	56	−14	5.08	333
	Parahippocampal gyrus (pHIPP)	R	20	−12	−34	4.98	428
	Frontal pole	R	42	58	−8	4.97	63
	Postcentral gyrus	R	60	−20	18	4.74	265
	Frontal orbital cortex	R	46	28	−18	4.54	43
	Visual cortex V3-V5	R	38	−86	−8	4.33	86
	Thalamus	L	−16	−20	18	4.18	122
	Frontal pole	L	−32	36	40	3.82	107
	Superior temporal gyrus	R	68	−16	−2	3.81	13
	Medial superior frontal gyrus (mSFG)	L/R	0	30	48	3.79	80
	Visual cortex V3-V5	L	−36	−84	−6	3.77	59
	Dorsolateral prefrontal cortex	L	−40	14	44	3.59	58
	Midbrain	L	−10	−22	−12	3.57	36
	Middle temporal gyrus	L	−56	−42	−8	3.51	27
	Supramarginal gyrus (SMG)	L	−42	−52	40	3.51	184
	Premotor cortex	R	34	16	46	3.47	23
	Temporal fusiform cortex	L	−32	−42	−10	3.45	99
	Medial superior frontal gyrus (mSFG)	L	−2	24	64	3.40	21
	Thalamus	L	−2	−20	10	3.36	19
	Middle temporal gyrus	R	68	−18	−16	3.34	11
	Precuneous	R	14	−60	22	3.34	23
	Frontal orbital cortex (FOC)	R	42	36	−6	3.33	50
	Visual cortex	R	18	−94	−8	3.29	26
	Temporal pole	L	−60	−2	−14	3.28	17
	Postcentral gyrus	R	56	−18	36	3.20	23
Task PLS	Medial superior frontal gyrus /anterior cingulate cortex (mSFG/ACC)	L	−4	4	56	15.89	27369
	Visual cortex (VIS)	L	−48	−70	2	12.86	19115
	Visual cortex (VIS)	R	32	−90	2	12.46	748
	Visual cortex (VIS)	R	28	−70	34	7.64	120
	Pons	L	−2	−28	−38	3.31	18
	Thalamus (THA)	L/R	0	−16	14	3.11	10

(Table continues.)

Table 1. Continued

Model	Region	HEM	MNI coordinates X	Y	Z	BSR	Cluster size (voxels)
	Posterior cingulate cortex (PCC)	L	−6	−50	28	−12.14	19444
	Visual cortex (VIS)	L	−54	−62	32	−11.49	1717
	Medial prefrontal cortex (mPFC)	L	−2	52	−8	−10.75	7702
	Planum temporale (PT)	R	58	−4	4	−9.07	8787
	Visual cortex (VIS)	R	52	−66	32	−7.69	826
	Frontal pole (FP)	R	52	38	0	−7.54	467
	Superior parietal lobule	R	26	−38	72	−4.51	112
	Insular cortex (INS)	R	36	4	8	−3.44	10

All peaks and clusters were determined using a voxel extent ≥10 and bootstrap ratio (BSR) ≥3.00. HEM, Hemisphere; MNI, Montreal Neurological Institute (mm); L, left; R, right.

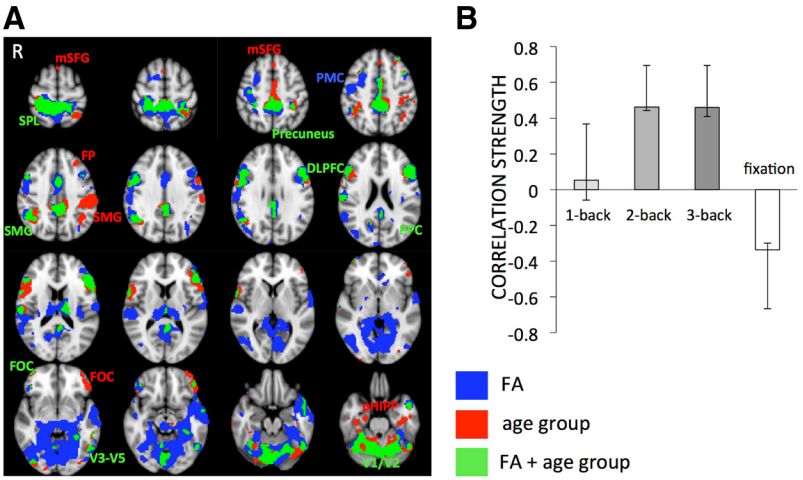

Figure 3. Spatial differences and similarities between FA-BOLD and age group-BOLD multivariate models. ***A***, Only FA-BOLD relations were predominant in the premotor, temporal, and visual regions, as well as in parts of DLPFC and thalamus (in blue). Age group-BOLD relations were robust in supramarginal, prefrontal, and parahippocampal regions (in red). FA-BOLD and age group-BOLD models overlapped in parietal, lateral prefrontal, posterior cingulate/precuneus, and visual regions (in green). The voxelwise spatial correlation of the first latent variables of the two models yielded Pearson $r = 0.72$, indicating that the two models shared only 52% spatial similarities. Labels are listed in Table 1. ***B***, Correlation magnitudes (Pearson *r*) between age group and BOLD signal during 1-, 2-, 3-back, and fixation (permuted $p < 0.001$, error bars represent bootstrapped 95% confidence intervals).

ginal, prefrontal, and parahippocampal regions. Regions where the age group-BOLD and FA-BOLD models overlapped included DLPFC, visual cortex, posterior cingulate gyrus/precuneus, and superior parietal lobule. Similar to the effect of FA on BOLD, the effect of age group on BOLD was significant only in conditions with sufficient working memory load (2- and 3-back; Fig. 3*B*). Though some regions representing the FA-BOLD relationship overlapped with the regions representing age group differences, the majority of the regions expressing the FA-BOLD association were common to both age groups.

FA-BOLD signal relationships during task and fixation

The results depicted in Figure 2 show that FA was negatively related to BOLD signal during task and positively related to BOLD signal during fixation. Corresponding regions included the frontoparietal control and dorsal attention areas, in which BOLD signal typically increases during task, as well as cingulo-parietal default regions, in which BOLD signal typically increases during fixation relative to task (Spreng, 2012). To more precisely identify n-back task-positive and -negative regions within this single spatial pattern (Fig. 2*A*), we performed a mean-centered task PLS analysis, which models how brain activity covaries with experimental conditions. Only one LV described the BOLD signal differences between task and fixation ($p < 0.001$, 94.09% crossblock covariance). Figure 4*A* shows that task-positive regions included premotor, medial prefrontal, anterior cingulate, DLPFC, frontopolar cortex, insula, caudate, thalamus, and visual areas, whereas the task-negative regions included precuneus, lateral occipital regions, medial PFC, fronto-orbital and posterior cingulate cortex, medial temporal lobe, and temporal pole. This pattern resembles closely that observed in previous fMRI studies on working memory (Rypma and D'Esposito, 1999; Cabeza and Nyberg, 2000; Mazoyer et al., 2001; Owen et al., 2005; Prakash et al., 2012b). To investigate how the FA-BOLD relations correspond to task-positive and task-negative regions, we overlaid the pattern of FA-BOLD correlations (Fig. 2*A*) and the spatial pattern map of the mean-centered task PLS (Fig. 4*A*). Figure 4*B* depicts the FA-BOLD relationship for task-positive regions, whereas Figure 4*C* depicts FA-BOLD correlations for task-negative regions.

To interpret the meaning of "higher BOLD signal" in these task-positive or task-negative regions, we examined the magnitude (%) of BOLD signal change. To this end, we used the clusters in Figure 4, *B* and *C*, as masks to extract the percent BOLD signal change from the functional images of each participant (i.e., from the three task conditions from clusters shown in Fig. 4*B*, and from fixation periods from clusters in Fig. 4*C*). We then regressed percent BOLD signal change on representative FA values (global FA) to visualize the sign and magnitude of BOLD signal change, as well as its relationship to FA. Higher global FA was related to smaller BOLD signal increases in task-positive regions ($r = -0.64$, $p < 0.001$, $n = 52$), and to greater BOLD signal increases in task-negative regions ($r = 0.51$, $p < 0.001$, $n = 52$). To further visualize discrete (i.e., task-positive and -negative) by continuous variable (FA) interactions on percent BOLD, we calculated point estimates based on ±1 SD from the whole-sample FA value (given the slope and intercept from the regression models) and plotted the interaction with task-positive and -negative regions. Figure 4*E* shows that BOLD signal changes during task and fixation were balanced in individuals with higher FA. In contrast, individuals with lower FA showed greater BOLD signal change during performance in task-positive regions, and reduced BOLD signal change during fixation in task-negative regions.

Finally, we compared the independent effects of age group and global FA on percent BOLD signal change. As shown in Table

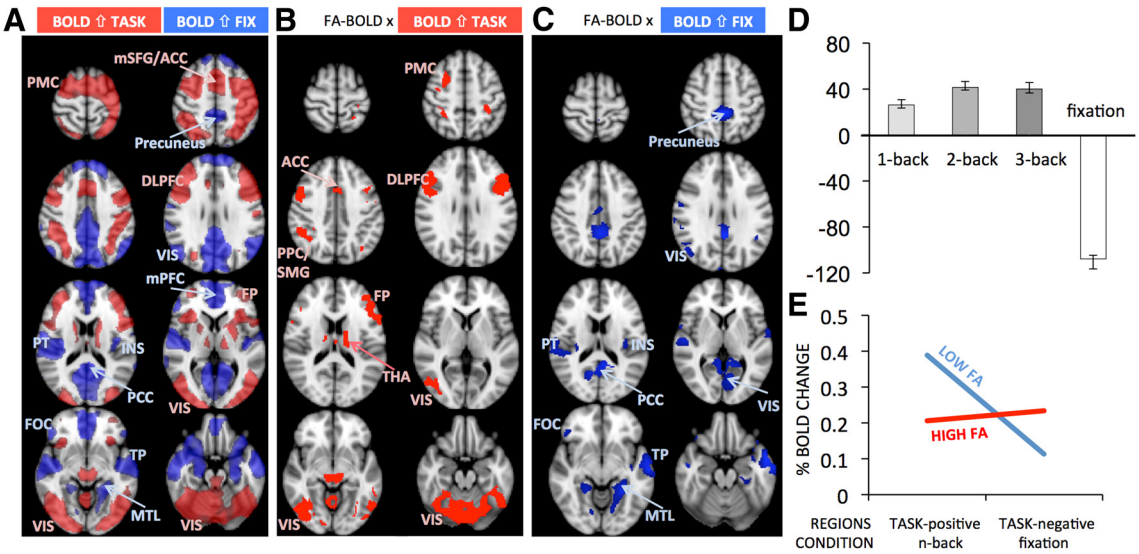

Figure 4. FA-BOLD relations for task-positive and task-negative BOLD signal. ***A***, Mean-centered PLS revealed regions where BOLD signal increased on task (in red) or increased during fixation (in blue). Task-positive regions included the typical frontoparietal working memory network, as well as visual, anterior cingulate, and subcortical regions, while task-negative regions revealed typical default-mode network regions. Region abbreviations are listed in Table 1. ***B***, FA-BOLD correlations within task-positive regions. ***C***, FA-BOLD correlations within task-negative regions. ***D***, Mean-centered brain scores showing differences from the mean of 1-, 2-, 3-back, and fixation (error bars represent bootstrapped 95% confidence intervals). ***E***, Schematic representation of the differences in percent BOLD signal change between adults with higher and lower FA. The point estimates were calculated based on ± 1 SD global FA values given the slope and intercept from regression Models 1 and 2 in Table 1.

Table 2. Regression models predicting brain activity and task performance

Dependent variables	Predictors	*t*	*p*	Partial η^2
1. TP % change	Global FA	−3.58	0.00	0.21
	Age group	1.26	0.21	0.03
2. TN % change	Global FA	2.97	0.01	0.15
	Age group	−0.28	0.78	0.00
3. N-back accuracy	Mean BS	3.53	0.00	0.20
	Age group	−3.46	0.00	0.20
4. N-back RT	Mean BS	−3.31	0.00	0.18
	Age group	1.46	0.15	0.04

BS, Brain score; TP, task positive; TN, task negative.

Table 3. Behavioral performance (n-back task)

	Working memory load	YA $n = 27$		OA $n = 28$		YA + OA $n = 55$	
		M	SD	M SD	SD	M	SD
Accuracy (% correct)	1-back	0.98	0.05	0.93	0.08	0.95	0.07
	2-back	0.92	0.06	0.81	0.09	0.86	0.09
	3-back	0.84	0.06	0.77	0.10	0.81	0.09
RT (ms)	1-back	705	94	815	120	761	121
	2-back	825	114	890	103	858	113
	3-back	821	100	887	97	854	103

M, Mean.

2, for both the task-positive regions (Model 1) and task-negative regions (Model 2), global FA predicted raw BOLD signal change beyond age group differences. The same results were obtained when using chronological age instead of age group in these analyses. These results suggest that FA is a better predictor than age group for BOLD signal changes either during fixation or during working memory performance.

Structure—function relations predict cognitive performance

Finally, we investigated whether the observed structure—function associations are behaviorally relevant. Mean and SDs for accuracy and reaction times are presented in Table 3. To relate structure—function associations to behavior, we correlated the average brain score (across the three n-back conditions) from our FA-BOLD multivariate model (Fig. 2) with average RT and accuracy (across the three n-back conditions). We averaged the values across conditions for two reasons. First, the error bars of the FA-BOLD correlations were overlapping for all three n-back conditions. Second, preliminary analyses (data not shown) showed a positive relationship between the brain scores and performance in each condition. Thus, correlating average n-back brain score and performance values was representative for the three conditions. Both correlations yielded significant results: Higher brain scores (i.e., higher FA and lower BOLD) were related to faster and more accurate n-back performance (Fig. 5)[a]. We then tested whether brain scores were related to performance after statistically controlling for age group differences. Table 2 depicts two general linear models with either accuracy (Model 3) or RT (Model 4) as dependent variables and task brain scores and age group as independent variables. Although both age group and brain scores independently predicted n-back accuracy, only the FA-BOLD brain scores accounted for a significant portion of the variance in RT. Again, the outcome was identical when chronological age was used in these analyses[b]. This indicates that FA-BOLD relations predict working memory performance independently of (both models) and better than (RT model) age group differences.

Discussion

We used a whole-brain, multivariate approach to investigate structure—function associations in the healthy adult brain. We

[a]Within-age-group analyses revealed a similar direction of correlation between FA-BOLD-based task brain score (BS) and mean n-back accuracy (YA: $r = 0.25$; OA: $r = 0.63$) and FA-BOLD-based task BS and mean n-back RT (YA: $r = -.21$; OA: $r = -.50$). Although effects within the YA group were weaker, Fisher's *r*-to-z transformation indicated that the correlation coefficients were not significantly different between the YA and OA groups (one-tailed, $p > 0.05$).

[b]We performed additional analyses using hit rate, false alarm rate, A′, and hit minus false alarm rate as measures of n-back performance, taking into account possible response bias and sensitivity. All these measures confirmed our accuracy-based results reported above.

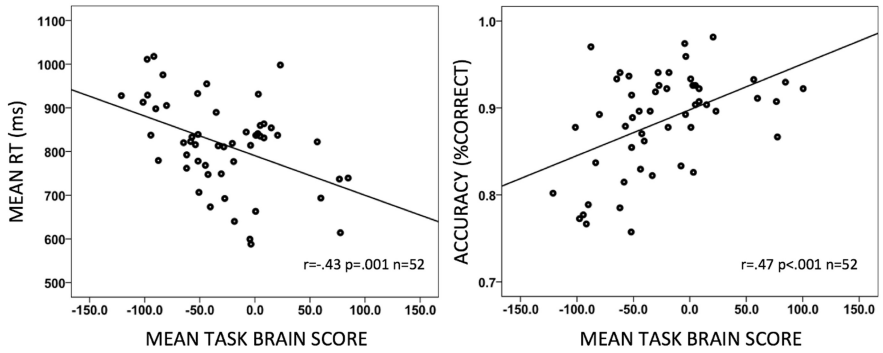

Figure 5. Structure–function relations predict working memory performance. The scatterplots depict correlations of mean task brain scores for FA-BOLD relations to RT and accuracy across the three n-back conditions. Higher brain scores refer to higher FA and lower BOLD signal.

obtained three main findings. First, higher WM microstructural integrity was related to BOLD signal in GM. Specifically, individuals with more intact WM showed less BOLD signal increase in task-positive regions (e.g., DLPFC) during task performance and more BOLD signal increase in task-negative regions (e.g., precuneus) during fixation. This relation was consistent across conditions and WM tracts, and spatially extended beyond age group differences in BOLD. Previously (Burzynska et al., 2011), we showed that task-specific adjustment of BOLD signal in restricted task-positive regions is related to properties of specific frontoparietal tracts in young adults. The current study extends these findings by demonstrating that the degree of recruiting whole-GM task-positive or -negative states is related to the integrity of all major WM tracts, and in a far more heterogeneous sample. Second, structure—function relations were reliable predictors of accuracy and latency. Third, the observed structure—function–behavior associations did not depend on variance related to age group. Together, our findings suggest that the structure—function properties of the adult brain underlie individual differences in cognition, and that WM integrity appears to be a better proxy of GM function and task performance than age group, even when using a broadly aged sample.

Higher FA and lower BOLD during task performance: a signature of neural efficiency?

As predicted, adults with greater integrity of anatomical connections showed lower BOLD signal increase in task-positive regions, and performed faster and more accurately on n-back. This pattern supports neural efficiency theory (Haier et al., 1988), indicating that better performing individuals use fewer brain energy resources to cope with task demands (Neubauer and Fink, 2009). This concept has been supported especially by working memory fMRI studies reporting lower and less extensive prefrontal activation in faster or more accurate young healthy adult performers (Rypma and D'Esposito, 1999; Rypma et al., 2002). Our study extends this concept by providing initial evidence of structural brain correlates of neural efficiency unconstrained by particular ROIs. Specifically, better quality of structural connections (higher FA) allows for more efficient use of GM resources on task (lower task-positive BOLD signal increases). In mature WM structures, higher FA is a proxy for larger axon caliber, higher density of myelinated axons, and thicker myelin (Beaulieu, 2002), which increase the speed of action potentials conduction along axons, resulting in faster or more robust communication between different GM regions (Fields, 2008). Although a number of studies showed a positive link between FA and cognitive performance in healthy adults (Johansen-Berg, 2010; Burzynska et al., 2011), especially in the context of aging (Madden et al., 2009, 2012), here we provide novel evidence for the link between WM microstructure and GM processing efficiency in general.

One conceptualization that helps relate WM integrity to higher processing efficiency may be the role of WM in processing speed (Salthouse, 1996; Deary, 2000; Jensen, 2006). Specifically, if poor WM integrity precludes fast and reliable signal transduction, the outputs of previous cognitive operations may no longer be synchronized with other outputs by the time they are delivered to the target regions via association fibers, thus inhibiting successful execution of subsequent cognitive operations [Salthouse's (1996) simultaneity and limited time principles]. This should result in lower quality and/or early degradation of mnemonic representations during encoding, and thus require more processing effort to maintain the memory contents during updating and retrieval (Myerson et al., 1990; Rypma and D'Esposito, 1999). In this sense, our results extend the simultaneity principle to individual differences in neural efficiency and cognitive performance.

A related link between WM integrity and BOLD signal could be that slower and less reliable signal transduction may exert more demands on cognitive control to ensure the integrity of interactions within task-related networks. For instance, Rypma et al. (2006) reported that slower performers showed more cortical activity especially in DLPFC and that PFC had more influence over other brain regions. Prakash et al. (2012a) demonstrated that acquiring complex skills by extensive videogame training resulted in improved game performance and reduced frontoparietal activity subserving attention and executive control. Similarly, we observed negative FA-BOLD correlations in frontoparietal regions, anterior cingulate, and frontopolar cortex, known as neural correlates of cognitive control (Dosenbach et al., 2007). The mechanisms relating WM structural connectivity to GM functional efficiency outlined above are not mutually exclusive: effortful processing of unsynchronized or lower quality representations may exert higher demands on cognitive control.

Importantly, our arguments regarding neural efficiency do not detract from our previous work showing that: (1) it is functional for select task-positive ROIs to "respond" via increased BOLD signal as working memory load increases; and, (2) the ability to modulate BOLD signal in this way is generally reduced in older/lower-performing adults. Importantly, older adults often exhibited higher ROI-based mean activation, possibly reflecting lower processing efficiency (Nagel et al., 2009, 2011). The direction of this effect converges with our current work, which highlights that neural efficiency could be considered as a generalized function of WM integrity (more so than age), GM function, and cognitive outcomes in a whole-brain context.

Neural efficiency as successful utilization of task-positive and task-negative states

Increased BOLD signal in task-positive regions during task performance, along with less BOLD signal during fixation, suggest a bias toward greater task-related GM activity in adults with lower WM integrity. McKiernan et al. (2003) demonstrated a greater magnitude of task-negative BOLD with increasing task difficulty, suggesting that task-induced "deactivations" represent reallocation of process-

ing resources to regions involved in performing the task. Later network analyses showed that the competition between networks (e.g., frontoparietal control and default networks) is necessary for mental flexibility and optimal performance (Raichle et al., 2001; Fox et al., 2005; Raichle and Snyder, 2007; Spreng, 2012). Our findings extend these observations by showing that individuals with better structural connectivity show comparable magnitudes of BOLD signal increase in task-positive regions during performance and in task-negative regions during fixation. This magnitude-balanced differentiation between states depending on cognitive demand may be a key feature for proficient working memory performance. Conversely, lower WM integrity may impair the communication between "competing" rest- and task-related states. This converges with higher engagement of task-positive regions and lower task-related deactivations observed in older adults (Sperling et al., 2009; Grady et al., 2010; Sambataro et al., 2010), who typically have reduced WM integrity (Burzynska et al., 2010).

Collectively, our results suggest that high quality of structural connectivity is needed for maintaining an ideally balanced differentiation between task-positive and task-negative neural activity. Relatedly, recent neurocomputational models demonstrated that there is an optimal range of conduction velocities that allows emergence of a network's spatiotemporal structure (Deco et al., 2011). For example, prototypical couplings disintegrate and global activity patterns reorganize when transmission velocities via anatomical connections are varied below the optimum (Ghosh et al., 2008; Deco et al., 2009), such as in case of compromised WM integrity. Effectively, these models predict that structural variability or integrity can preclude healthy brain function, perhaps serving as a generalized model under which our present findings may be extended in future work.

WM integrity: a better proxy of function and performance than age

We showed that WM integrity is a better proxy of GM activity than age group, and structure—function brain properties predict performance beyond age group. Thus, the adult lifespan could be perceived as a condition of heterogeneity in neural efficiency, resulting from individual differences in brain structural and functional properties, as well as individual differences in the rate of age-related degradation of biological resources (Lindenberger et al., 2013; Nyberg et al., 2012). The predictive power of WM integrity in our data converges with studies highlighting the importance of defining "biological age" (for which FA could be a proxy) to more appropriately describe developmental processes of brain function and cognition, rather than more indirect proxies such as chronological age (MacDonald et al., 2004, 2011). Relatedly, the concept of cortical disconnection due to breakdown of WM tracts has been proposed as a mechanism accounting for age-related cognitive decline (Andrews-Hanna et al., 2007; Kennedy and Raz, 2009), and could be extended to ideas about structural connectivity-bound GM efficiency. Some spatial overlap of the effects of age group and FA on BOLD signal could be accounted for by other modulators of GM activity, such as age-related depletion in the dopaminergic system (Bäckman et al., 2010); future work could consider this possibility.

Conclusions

Our study demonstrates that individual differences in the integrity of major WM tracts are related to individual differences in whole-GM task-positive and -negative activity. Negative relations between WM integrity and task-related BOLD signal suggest that better quality of structural connections allows for more efficient use of GM-processing resources during performance and optimal differentiation between task-positive and task-negative states. Importantly, these structural–functional brain properties continued to predict accuracy and latency after controlling for age. Finally, our study demonstrated a viable approach for examining the whole-brain multivariate combination of DTI and fMRI data. Our cross-sectional results should be followed-up longitudinally to investigate lead-lag relations of structural and functional brain changes, and their relations to cognitive functioning, across the lifespan.

References

Andersson JLR, Jenkinson M, Smith S (2007) Non-linear registration aka spatial normalization. FMRIB Tech Rep TR07JA2.

Andrews-Hanna JR, Snyder AZ, Vincent JL, Lustig C, Head D, Raichle ME, Buckner RL (2007) Disruption of large-scale brain systems in advanced aging. Neuron 56:924–935. CrossRef Medline

Bäckman L, Lindenberger U, Li SC, Nyberg L (2010) Linking cognitive aging to alterations in dopamine neurotransmitter functioning: recent data and future avenues. Neurosci Biobehav Rev 34:670–677. CrossRef Medline

Beaulieu C (2002) The basis of anisotropic water diffusion in the nervous system—a technical review. NMR Biomed 15:435–455. CrossRef Medline

Bollen KA, Jackman RW (1990) Regression diagnostics: an expository treatment of outliers and influential cases. In: Modern methods of data analysis (Fox J, Long J S, eds), pp 257–91. Newbury Park, CA: Sage.

Buckner RL, Andrews-Hanna JR, Schacter DL (2008) The brain's default network: anatomy, function, and relevance to disease. Ann N Y Acad Sci 1124:1–38. CrossRef Medline

Burzynska AZ, Preuschhof C, Bäckman L, Nyberg L, Li SC, Lindenberger U, Heekeren HR (2010) Age-related differences in white matter microstructure: Region-specific patterns of diffusivity. Neuroimage 49:2104–2112. CrossRef Medline

Burzynska AZ, Nagel IE, Preuschhof C, Li SC, Lindenberger U, Bäckman L, Heekeren HR (2011) Microstructure of frontoparietal connections predicts cortical responsivity and working memory performance. Cereb Cortex 21:2261–2271. CrossRef Medline

Cabeza R, Nyberg L (2000) Neural bases of learning and memory: functional neuroimaging evidence. Curr Opin Neurol 13:415–421. CrossRef Medline

Deary IJ (2000) Looking down on human intelligence: from psychometrics to the brain. New York: Oxford UP.

Deco G, Jirsa V, McIntosh AR, Sporns O, Kötter R (2009) Key role of coupling, delay, and noise in resting brain fluctuations. Proc Natl Acad Sci U S A 106:12207–12208. CrossRef

Deco G, Jirsa VK, McIntosh AR (2011) Emerging concepts for the dynamical organization of resting-state activity in the brain. Nat Rev Neurosci 12:43–56. CrossRef Medline

Dosenbach NU, Fair DA, Miezin FM, Cohen AL, Wenger KK, Dosenbach RA, Fox MD, Snyder AZ, Vincent JL, Raichle ME, Schlaggar BL, Petersen SE (2007) Distinct brain networks for adaptive and stable task control in humans. Proc Natl Acad Sci U S A 104:11073–11078. CrossRef Medline

Efron B, Tibshirani RJ (1993) An introduction to the bootstrap. London: Chapman and Hall.

Fields RD (2008) White matter in learning, cognition and psychiatric disorders. Trends Neurosci 31:361–370. CrossRef Medline

Fjell AM, Westlye LT, Amlien IK, Walhovd KB (2011) Reduced white matter integrity is related to cognitive instability. J Neurosci 31:18060–18072. CrossRef Medline

Fox MD, Snyder AZ, Vincent JL, Corbetta M, Van Essen DC, Raichle ME (2005) The human brain is intrinsically organized into dynamic, anticorrelated functional networks. Proc Natl Acad Sci U S A 102:9673–9678. CrossRef Medline

Ghosh A, Rho Y, McIntosh AR, Kötter R, Jirsa VK (2008) Noise during rest enables the exploration of the brain's dynamic repertoire. PLoS Comput Biol 4:e1000196. CrossRef Medline

Grady CL, Springer MV, Hongwanishkul D, McIntosh AR, Winocur G (2006) Age-related changes in brain activity across the adult lifespan. J Cogn Neurosci 18:227–241. CrossRef Medline

Grady CL, Protzner AB, Kovacevic N, Strother SC, Afshin-Pour B, Wojtowicz M, Anderson JA, Churchill N, McIntosh AR (2010) A multivariate analysis of age-related differences in default mode and task-positive networks across multiple cognitive domains. Cereb Cortex 20:1432–1447. CrossRef Medline

Haier RJ, Siegel BV, Nuechterlein KH, Hazlett E, Wu JC, Paek J, Browning HL, Buchsbaum MS (1988) Cortical glucose metabolic rate correlates of abstract reasoning and attention studied with positron emission tomography. Intelligence 12:199–217. CrossRef

Hofer S, Frahm J (2006) Topography of the human corpus callosum revisited–comprehensive fiber tractography using diffusion tensor magnetic resonance imaging. Neuroimage 32:989–994. CrossRef Medline

Jenkinson M, Smith S (2001) A global optimisation method for robust affine registration of brain images. Med Image Anal 5:143–156. CrossRef Medline

Jenkinson M, Bannister P, Brady M, Smith S (2002) Improved optimization for the robust and accurate linear registration and motion correction of brain images. Neuroimage 17:825–841. CrossRef Medline

Jensen AR (2006) Clocking the mind: mental chronometry and individual differences. Amsterdam: Elsevier.

Johansen-Berg H (2010) Behavioural relevance of variation in white matter microstructure. Curr Opin Neurol 23:351–358. Medline

Kennedy KM, Raz N (2009) Aging white matter and cognition: differential effects of regional variations in diffusion properties on memory, executive functions, and speed. Neuropsychologia 47:916–927. CrossRef Medline

Krishnan A, Williams LJ, McIntosh AR, Abdi H (2011) Partial Least Squares (PLS) methods for neuroimaging: a tutorial and review. Neuroimage 56:455–475. CrossRef Medline

Lindenberger U, Burzynska AZ, Nagel IE (2013) Heterogeneity in frontal lobe aging. In: Principles of frontal lobe functions (Stuss DT, Knight RT, eds), Ed 2, pp 609–627. New York: Oxford UP.

Lustig C, Snyder AZ, Bhakta M, O'Brien KC, McAvoy M, Raichle ME, Morris JC, Buckner RL (2003) Functional deactivations: change with age and dementia of the Alzheimer type. Proc Natl Acad Sci U S A 100:14504–14509. CrossRef Medline

MacDonald SW, Dixon RA, Cohen AL, Hazlitt JE (2004) Biological age and 12-year cognitive change in older adults: findings from the Victoria Longitudinal Study. Gerontology 50:64–81. CrossRef Medline

MacDonald SW, DeCarlo CA, Dixon RA (2011) Linking biological and cognitive aging: toward improving characterizations of developmental time. J Gerontol B Psychol Sci Soc Sci 66 [Suppl 1]:i59–i70.

Madden DJ, Spaniol J, Whiting WL, Bucur B, Provenzale JM, Cabeza R, White LE, Huettel SA (2007) Adult age differences in the functional neuroanatomy of visual attention: a combined fMRI and DTI study. Neurobiol Aging 28:459–476. CrossRef Medline

Madden DJ, Bennett IJ, Song AW (2009) Cerebral white matter integrity and cognitive aging: contributions from diffusion tensor imaging. Neuropsychol Rev 19:415–435. CrossRef Medline

Madden DJ, Bennett IJ, Burzynska A, Potter GG, Chen NK, Song AW (2012) Diffusion tensor imaging of cerebral white matter integrity in cognitive aging. Biochim Biophys Acta 1822:386–400. Medline

Mazoyer B, Zago L, Mellet E, Bricogne S, Etard O, Houdé O, Crivello F, Joliot M, Petit L, Tzourio-Mazoyer N (2001) Cortical networks for working memory and executive functions sustain the conscious resting state in man. Brain Res Bull 54:287–298. CrossRef Medline

McIntosh AR, Lobaugh NJ (2004) Partial least squares analysis of neuroimaging data: applications and advances. Neuroimage 23 [Suppl 1]:S250–S63. Medline

McIntosh AR, Bookstein FL, Haxby JV, Grady CL (1996) Spatial pattern analysis of functional brain images using partial least squares. Neuroimage 3:143–157. CrossRef Medline

McKiernan KA, Kaufman JN, Kucera-Thompson J, Binder JR (2003) A parametric manipulation of factors affecting task-induced deactivation in functional neuroimaging. J Cogn Neurosci 15:394–408. CrossRef Medline

Mori S, Wakana S, Nagae-Poetscher LM, van Zijl PCM (2005) MRI atlas of human white matter. Amsterdam: Elsevier Science.

Myerson J, Hale S, Wagstaff D, Poon LW, Smith GA (1990) The information-loss model: a mathematical theory of age-related cognitive slowing. Psychol Rev 97:475–487. CrossRef Medline

Nagel IE, Preuschhof C, Li SC, Nyberg L, Bäckman L, Lindenberger U, Heekeren HR (2009) Performance level modulates adult age differences in brain activation during spatial working memory. Proc Natl Acad Sci U S A 106:22552–22557. CrossRef Medline

Nagel IE, Preuschhof C, Li SC, Nyberg L, Bäckman L, Lindenberger U, Heekeren HR (2011) Load modulation of BOLD response and connectivity predicts working memory performance in younger and older adults. J Cogn Neurosci 23:2030–2045. CrossRef Medline

Neubauer AC, Fink A (2009) Intelligence and neural efficiency. Neurosci Biobehav Rev 33:1004–1023. CrossRef Medline

Nyberg L, Lövdén M, Riklund K, Lindenberger U, Bäckman L (2012) Memory aging and brain maintenance. Trends Cogn Sci 16:292–305. Medline

Owen AM, McMillan KM, Laird AR, Bullmore E (2005) N-back working memory paradigm: a meta-analysis of normative functional neuroimaging studies. Hum Brain Mapp 25:46–59. CrossRef Medline

Persson J, Nyberg L, Lind J, Larsson A, Nilsson LG, Ingvar M, Buckner RL (2006) Structure–function correlates of cognitive decline in aging. Cereb Cortex 16:907–915. Medline

Prakash RS, De Leon AA, Mourany L, Lee H, Voss MW, Boot WR, Basak C, Fabiani M, Gratton G, Kramer AF (2012a) Examining neural correlates of skill acquisition in a complex videogame training program. Front Hum Neurosci 6:115. Medline

Prakash RS, Heo S, Voss MW, Patterson B, Kramer AF (2012b) Age-related differences in cortical recruitment and suppression: Implications for cognitive performance. Behav Brain Res 230:192–200. CrossRef Medline

Raichle ME (2010) Two views of brain function. Trends Cogn Sci 14:180–190. CrossRef Medline

Raichle ME, Snyder AZ (2007) A default mode of brain function: a brief history of an evolving idea. Neuroimage 37:1083–1090; discussion 1097–1099. CrossRef Medline

Raichle ME, MacLeod AM, Snyder AZ, Powers WJ, Gusnard DA, Shulman GL (2001) A default mode of brain function. Proc Natl Acad Sci U S A 98:676–682. CrossRef Medline

Reese TG, Heid O, Weisskoff RM, Wedeen VJ (2003) Reduction of eddy-current-induced distortion in diffusion MRI using a twice-refocused spin echo. Magn Reson Med 49:177–182. CrossRef Medline

Rueckert D, Sonoda LI, Hayes C, Hill DL, Leach MO, Hawkes DJ (1999) Nonrigid registration using free-form deformations: application to breast MR images. IEEE Trans Med Imaging 18:712–721. CrossRef Medline

Rypma B, D'Esposito M (1999) The roles of prefrontal brain regions in components of working memory: effects of memory load and individual differences. Proc Natl Acad Sci U S A 96:6558–6563. CrossRef Medline

Rypma B, Berger JS, D'Esposito M (2002) The influence of working-memory demand and subject performance on prefrontal cortical activity. J Cogn Neurosci 14:721–731. CrossRef Medline

Rypma B, Berger JS, Prabhakaran V, Bly BM, Kimberg DY, Biswal BB, D'Esposito M (2006) Neural correlates of cognitive efficiency. Neuroimage 33:969–979. CrossRef Medline

Salthouse TA (1996) The processing-speed theory of adult age differences in cognition. Psychol Rev 103:403–428. CrossRef Medline

Sambataro F, Murty VP, Callicott JH, Tan HY, Das S, Weinberger DR, Mattay VS (2010) Age-related alterations in default mode network: impact on working memory performance. Neurobiol Aging 31:839–852. CrossRef Medline

Schulze ET, Geary EK, Susmaras TM, Paliga JT, Maki PM, Little DM (2011) Anatomical correlates of age-related working memory declines. J Aging Res 2011:606871. Medline

Smith SM (2002) Fast robust automated brain extraction. Hum Brain Mapp 17:143–155. CrossRef Medline

Smith SM, Jenkinson M, Woolrich MW, Beckmann CF, Behrens TEJ, Johansen-Berg H, Bannister PR, De Luca M, Drobnjak I, Flitney DE, Niazy RK, Saunders J, Vickers J, Zhang Y, De Stefano N, Brady JM, Matthews PM (2004) Advances in functional and structural MR image analysis and implementation as FSL. Neuroimage [Suppl 1]:S208–S219. Medline

Smith SM, Jenkinson M, Johansen-Berg H, Rueckert D, Nichols TE, Mackay CE, Watkins KE, Ciccarelli O, Cader MZ, Matthews PM, Behrens TE (2006) Tract-based spatial statistics: voxelwise analysis of multi-subject diffusion data. Neuroimage 31:1487–1505. CrossRef

Smith SM, Johansen-Berg H, Jenkinson M, Rueckert D, Nichols TE, Miller KL, Robson MD, Jones DK, Klein JC, Bartsch AJ, Behrens TE (2007) Acquisition and voxelwise analysis of multi-subject diffusion data with tract-based spatial statistics. Nat Protoc 2:499–503. CrossRef Medline

Sperling RA, Laviolette PS, O'Keefe K, O'Brien J, Rentz DM, Pihlajamaki M, Marshall G, Hyman BT, Selkoe DJ, Hedden T, Buckner RL, Becker JA, Johnson KA (2009) Amyloid deposition is associated with impaired default network function in older persons without dementia. Neuron 63:178–188. CrossRef Medline

Spreng RN (2012) The fallacy of a "task-negative" network. Front Psychol 3:145. Medline